Postcranial Pneumaticity and Bone Structure in Two Clades of Neognath Birds

SARAH C. GUTZWILLER,[1,2] ANNE SU,[3] AND PATRICK M. O'CONNOR[2,4]*
[1]Honors Tutorial College, Ohio University, Athens, Ohio
[2]Ohio Center for Ecology and Evolutionary Studies, Ohio University, Athens, Ohio
[3]College of Sciences and Health Professions, Cleveland State University, Cleveland, Ohio
[4]Department of Biomedical Sciences, Ohio University Heritage College of Osteopathic Medicine, Athens, Ohio

ABSTRACT

Most living birds exhibit some degree of postcranial skeletal pneumaticity, aeration of the postcranial skeleton by pulmonary air sacs and/or directly from the lungs. The extent of pneumaticity varies greatly, ranging from taxa that are completely apneumatic to those with air filling most of the postcranial skeleton. This study examined the influence of skeletal pneumatization on bone structural parameters in a sample of two size- and foraging-style diverse (e.g., subsurface diving vs. soaring specialists) clades of neognath birds (charadriiforms and pelecaniforms). Cortical bone thickness and trabecular bone volume fraction were assessed in one cervical and one thoracic vertebra in each of three pelecaniform and four charadriiform species. Results for pelecaniforms indicate that specialized subsurface dive foragers (e.g., the apneumatic anhinga) have thicker cortical bone and a higher trabecular bone volume fraction than their non-diving clademates. Conversely, the large-bodied, extremely pneumatic brown pelican *(Pelecanus occidentalis)* exhibits thinner cortical bone and a lower trabecular bone volume fraction. Such patterns in bone structural parameters are here interpreted to pertain to decreased buoyancy in birds specialized in subsurface dive foraging and decreased skeletal density (at the whole bone level) in birds of larger body size. The potential to differentially pneumatize the postcranial skeleton and alter bone structure may have played a role in relaxing constraints on body size evolution and/or habitat exploitation during the course of avian evolution. Notably, similar patterns were not observed within the equally diverse charadriiforms, suggesting that the relationship between pneumaticity and bone structure is variable among different clades of neognath birds. Anat Rec, 296:867–876, 2013.

Key words: pneumaticity; cortical bone; trabecular bone; Pelecaniformes; Charadriiformes; microcomputed tomography (μCT)

Grant sponsor: Ohio University Heritage College of Osteopathic Medicine; Grant sponsor: Ohio University Office of Research and Sponsored Programs.

*Correspondence to: Patrick M. O'Connor, Department of Biomedical Sciences, 228 Irvine Hall, Ohio University Heritage College of Osteopathic Medicine, Athens, OH 45701. E-mail: oconnorp@ohio.edu

Received 3 March 2012; Accepted 4 February 2013.
DOI 10.1002/ar.22691
Published online 1 April 2013 in Wiley Online Library (wileyonlinelibrary.com).

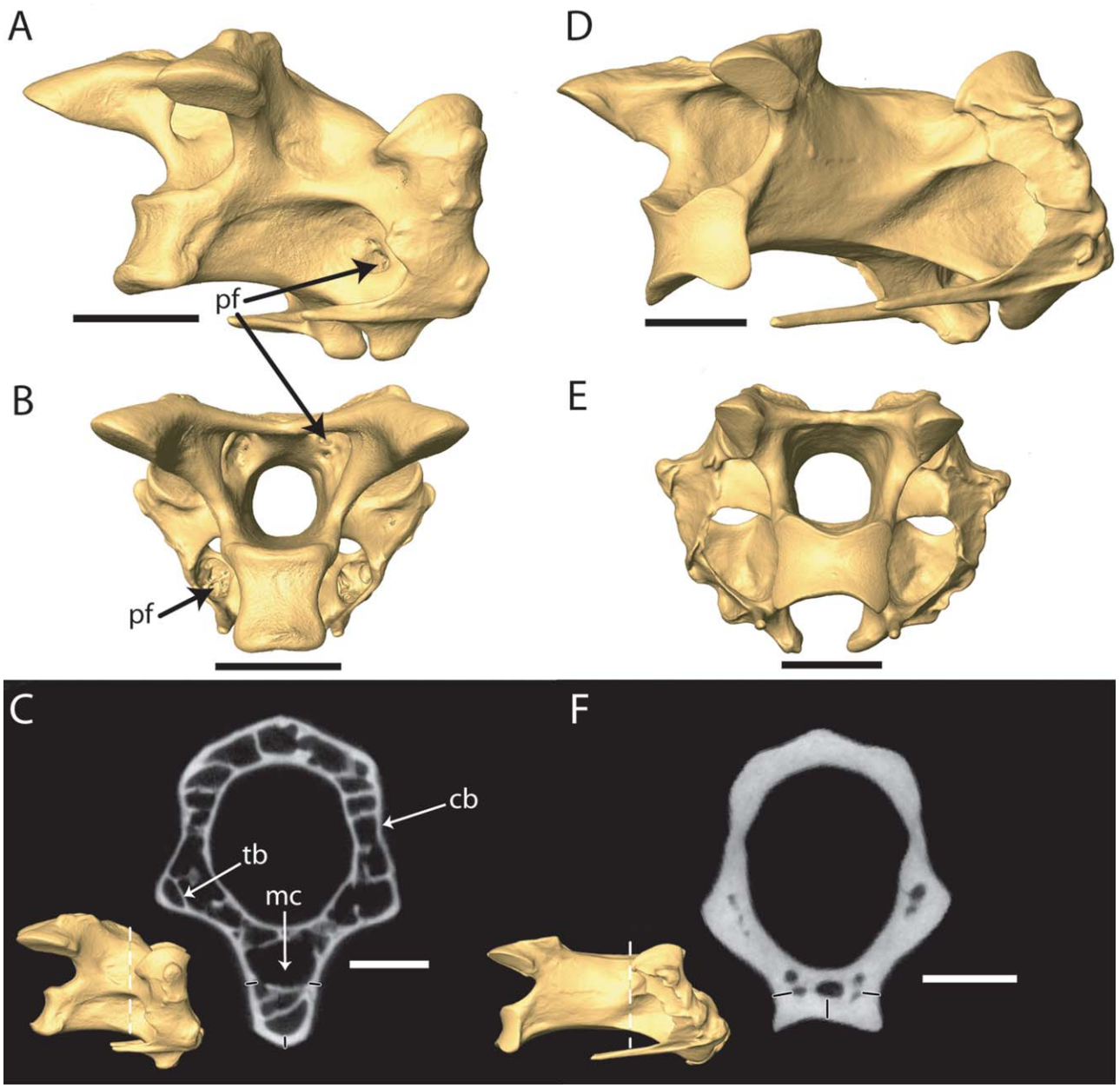

Fig. 1. Pneumatic cervical vertebra of *Catharacta skua* (CM 10116) in right oblique caudolateral (**A**) and caudal (**B**) views. **C**: Micro-computed tomography (μCT) scan cross-sectional slice of the pneumatic cervical vertebra of CM 10116, denoting cortical bone, trabecular bone, and the medullary cavity. Inset lateral view with white dashed line denotes the location of μCT cross-sectional slice in (C). Apneumatic cervical vertebra of *Phalocrocorax auritus* (OUVC 9772) in right oblique caudolateral (**D**) and caudal (**E**) views. **F**: μCT scan cross-sectional slice of the apneumatic cervical vertebra of OUVC 9772. Inset lateral view with white dashed line denotes the location of μCT cross-sectional slice in (F). Black lines with white outlines in (C) and (F) indicate location for Cb.T measurements in pneumatic (C) and apneumatic (F) vertebrate. 3D renderings created in Amira 4.1 using reconstructed μCT scans. Scale: 0.5 cm (A,B,D,E) and 0.25 cm (C and F). Abbreviations: mc, medullary cavity; pf, pneumatic foramen; cb, cortical bone; tb, trabecular bone.

Postcranial skeletal pneumatization is the process of aeration of the postcranial skeleton by the pulmonary air sacs and lungs (Duncker, 1971, 2004; O'Connor, 2004). It has been well-documented in certain groups of living birds (O'Connor, 2004, 2009; Smith, 2012) and inferred in a number of extinct archosaurs (e.g., saurischian dinosaurs and pterosaurs) (Wedel, 2003; O'Connor, 2006; Benson et al., 2012). Subsequent to hatching, epithelial-lined outgrowths of the air sacs, termed intraosseous pneumatic diverticula, penetrate the cortical bone through foramina or sutures (Bremer, 1940; Hogg, 1984; Witmer, 1990; O'Connor, 2004). Air sac and/or diverticular infiltration of the skeleton is marked by the characteristic presence of pneumatic foramina in bones (Fig. 1A,B). Marrow is displaced within the medullary cavity as diverticula enter the bone, leaving the bone

primarily filled with air (Bremer, 1940; Schepelmanm, 1990; Duncker, 2004). During this process it is thought that some trabecular bone within and cortical bone adjacent to the medullary cavity is resorbed (Bremer, 1940; Bellairs and Jenkin, 1960).

Research on extinct archosaurs, including sauropod and theropod dinosaurs and pterosaurs, has emphasized the importance of postcranial pneumaticity for the evolution of body size (Carrano and O'Connor, 2005; Wedel, 2005; O'Connor, 2006, 2009; Claessens et al., 2009; Benson et al., 2012). For example, many sauropod dinosaurs exhibit evidence of extensive pneumaticity of the axial skeleton that would have resulted in decreased bone mass. This has been interpreted as a mechanism allowing for the large body size attained by members of the clade (Sander et al., 2001; Wedel, 2005; Schwarz-Wings et al., 2010).

Recent research on birds, the only living sauropsid group to exhibit air-filled postcranial bones, suggests that specializations related to foraging and locomotion may have been influenced by the evolution of pneumaticity in this group (O'Connor, 2004, 2009; Smith, 2012). Select clades of living birds exhibit extensive pneumatization of the postcranial skeleton (including distal portions of the limbs), whereas others are completely apneumatic. The majority of neognath birds exhibit a moderate degree of postcranial skeletal pneumaticity, focused mostly within elements of the vertebral column (O'Connor, 2006). Variability in the extent of pneumaticity has been related to the variety of body sizes and foraging strategies observed in birds. For example, birds of large body size that employ specialized flight behaviors (e.g., static soaring in pelicans and vultures) tend to be extremely pneumatic (e.g., O'Connor, 2009). It has been suggested that pneumatization in such forms provides a mechanism that alters standard mass–volume relationships that most nonaquatic amniotes are subject to, allowing certain clades of volant birds to attain larger body sizes (i.e., whole-body volume) and exploit different niches. As a point of contrast, birds across multiple clades specialized for subsurface dive-foraging tend to have apneumatic or extremely reduced levels of pneumaticity within the postcranial skeleton relative to their non-diving clademates (O'Connor, 2004, 2009; Smith, 2012). In this case, the absence of air in the skeleton has been interpreted to allow diving birds to maintain neutral buoyancy under the water, allowing for more energetically efficient underwater locomotion.

Whereas large scale patterns of the evolution of pneumaticity are becoming evident at interspecific levels in certain clades, less well understood is how pneumatization affects bone structure and strength. Most previous research has focused on the effects of pneumatization on cortical bone. Pneumatic long bones tend to have a decreased relative cortical bone thickness (Cb.T), and a lower (1) bending strength (failure point) and (2) flexural Young's modulus when compared to apneumatic bones, suggesting that pneumatic bones have decreased biomechanical strength brought about by relatively thinner cortices (Kafka, 1983; Currey and Alexander, 1985; Cubo and Casinos, 1999). The widespread prevalence of pneumatic bones in many species of birds, even with the documented decrease in size-adjusted bending strength (e.g., Cubo and Casinos, 1999), suggests that there has been a selective advantage for pneumatizing the skeleton. With this apparent tradeoff of decreased biomechanical strength, pneumaticity decreases body mass not only by filling the medullary cavity with air instead of marrow, but also by initiating a decrease in skeletal mass brought about by resorption along the endosteal surface of the cortical bone (Bremer, 1940; Smith, et al., 2005). This decreased body mass may provide an energetic benefit during extended flight. In contrast, thicker cortical bone in the apneumatic vertebrae of dive foragers may act to reduce the amount of low-density bone marrow and increase skeletal mass as a means of reaching neutral buoyancy during diving (Fajardo et al., 2007). Thus, it seems that the energetic benefits associated with the presence of air vs. bone marrow may be increased by the observed differences in Cb.T.

Additional work has considered the impact of pneumatization on structural characteristics in trabecular bone in birds. Fajardo et al. (2007) conducted a pilot study on two anseriform (ducks, geese, swans) birds, one (*Aix sponsa*) exhibiting a pneumatic skeleton with the other (*Oxyura jamaicensis*) representing a completely apneumatic species. Contrary to predictions and generalizations already promoted in the literature (see, Bremer, 1940; Bellairs and Jenkin, 1960), there were no significant differences across a variety of trabecular bone parameters (trabecular bone volume to total volume fraction, structural anisotropy, etc.). To assess the generalized nature of the impact of pneumatization on cortical and trabecular bone structure, the present study was designed to examine attributes of both facets in two additional clades of neognath birds, Charadriiformes and Pelecaniformes.

MATERIALS AND METHODS

Specimens examined in this study were obtained from the collections at the Ohio University Vertebrate Collection (OUVC), Carnegie Museum of Natural History (CM), and the Smithsonian National Museum of Natural History (NMNH). The study sample included four charadriiforms spanning a wide range of body masses and exhibiting variability with regard to both foraging behavior (e.g., subsurface dive foragers vs. static soaring specialists) and the relative degree of postcranial skeletal pneumaticity (Table 1): the Common Murre (*Uria aalge*, a dedicated diver), the Atlantic Puffin (*Fratercula arctica*, a dedicated diver), the Western Gull (*Larus occidentalis*, a generalized flier), and the Great Skua (*Cathracta skua/maccormicki*, a soaring specialist). We also profiled bone characteristics in three pelecaniforms (Table 1): the Anhinga (*Anhinga anhinga*, a dedicated diver), the Double-crested cormorant (*Phalacrocorax auritus*, a dedicated diver), and the Brown Pelican (*Pelecanus occidentalis*, a soaring specialist).

Micro-Computed Tomography

One middle cervical (i.e., between cervical vertebra 9 and cervical vertebra 11; region II of Boas (1929) and Zusi (1962)) and one free thoracic vertebra (i.e., one from the cranial end of the thoracic series that is not fused with adjacent vertebrae) from six specimens of each species were scanned using a GE eXplore Locus micro-computed tomography scanner (GE Healthcare Pre-Clinical Imaging, London, ON,

TABLE 1. Focal Species Details[a]

Clade	Species	Mean BM (g)	Vertebrae pneumatic	Foraging specialization
Charadriiforms	*Uria aalge*	993	N	Dedicated diver
	Fractercula arctica	381	N	Dedicated diver
	Larus occidentalis	1011	Y	Generalized flier
	Catharacta skua	446	Y	Soaring specialist
Pelecaniforms	*Anhinga anhinga*	1235	N	Dedicated diver
	Phalocrocorax auritus	1674	N	Dedicated diver
	Pelecanus occidentalis	3438	Y	Soaring specialist

[a]Body mass data from Dunning (2007).

Canada) housed at Ohio University. All scans were acquired at an X-ray tube voltage of 80 kV, a current of 450 μA, and an effective voxel size of 0.045 mm. GE Microview software (GE Healthcare, http://microview.sourceforge.net) was used to optimize file size and export images in DICOM format. The image volumes were then imported into Amira 4.1 visualization software (Visage Imaging, San Diego, CA) for quantitative analyses. In the analysis of the following bone parameters, cortical bone was defined as bone exterior to the medullary cavity, whereas trabecular bone was defined as any bone within the medullary cavity (Fig. 1C).

Cortical bone thickness. An average Cb.T was calculated for each vertebra using Amira 4.1. In order to sample a homologous location among the species, we identified the cross-section located at the caudal end of the cranial zygapophyseal facet (Fig. 1C,F). To attain an overall estimate of Cb.T at this location, three separate Cb.T measurements were acquired, one at the ventral midline and one along each lateral margin of the centrum at mid-centrum height (Fig. 1F). In order to account for local irregularities, these three measurements were averaged to obtain a mean centrum Cb.T. The mean thickness was then standardized by dividing by the species mean body mass (Table 1; Dunning, 2007).

Trabecular bone volume fraction. An estimate of trabecular bone volume fraction (BV/TV) was calculated for a homologous region located just caudal to the cranial articular facet of each vertebra. To determine BV/TV, a spherical volume of interest (VOI) was established within the medullary cavity at this region using Amira 4.1 (Fig. 2A). To ensure that only trabecular bone was included, the maximum diameter of the VOI extended to the junction of the cortical and trabecular bone (Fig. 2B,C). This VOI was imported into Quant3D (University of Texas; Ketcham and Ryan, 2004) following protocols outlined by Ketcham and Ryan (2004) and Cotter et al. (2009). In Quant3D, trabecular bone in the VOI was binarized into bone/non-bone using an adaptive, iterative threshold technique (Ridler and Calvard, 1978), with BV/TV estimated using the star volume distribution (SVD) algorithm (Cruz-Orive et al., 1992; Ketcham and Ryan, 2004). Individual BV/TV values were averaged to attain mean BV/TV for each species for each of the two vertebrae examined.

Statistical approaches. Species mean values and coefficients of variation (CoV) for the two bone parameters (Cb.T and BV/TV) were calculated. In PASW 18, Kruskall–Wallis (K independent samples) tests were performed to identify significant differences in the two bone structural parameters among all species within an order. Subsequently, Mann–Whitney (pairwise, two-independent samples) tests were used to compare species within an order in a pairwise fashion. Mann–Whitney tests were also performed to identify intraspecific differences in bone structure between cervical and thoracic vertebrae. Kruskall–Wallis and Mann–Whitney tests were used due to the small sample sizes in this study and as is standard in other studies of this nature with comparable sample sizes (e.g., Fajardo et al., 2007).

RESULTS

Tables 2 (pelecaniformes) and 3 (charadriiformes) summarize the bone structural results for each species examined in the study. Raw values for all examined specimens are reported in the Appendix. Cb.T was significantly higher in *Anhinga* and *Phalacrocorax* relative to *Pelecanus* ($P < 0.05$) for both cervical and thoracic vertebrae (Fig. 3A). BV/TV was also significantly higher in *Anhinga* and *Phalacrocorax* relative to *Pelecanus* ($P < 0.05$) for thoracic vertebrae, with no significant differences identified in BV/TV ($P = 0.073$) for cervical vertebrae (Fig. 3B). The highest coefficient of variation within pelecaniforms was in the cervical BV/TV for *Pelecanus* (CoV = 0.51). Within individual pelecaniform species, there were no significant differences in Cb.T or BV/

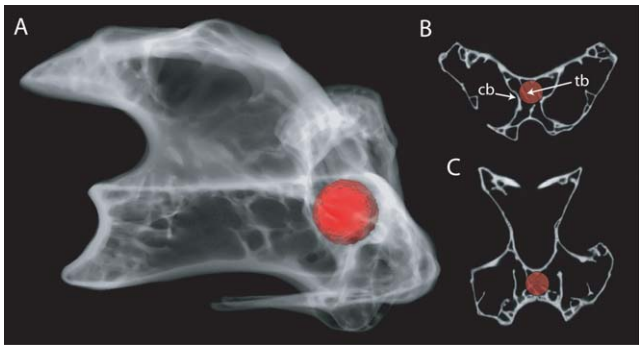

Fig. 2. **A**: Cervical vertebra of *Catharacta maccormicki* (USNM 554803) in right lateral projection view, denoting the location of the spherical VOI used to assess trabecular bone volume fraction. μCT cross-sectional slices in craniocaudal (**B**) and dorsoventral (**C**) projections indicating the location of the VOI. Abbreviations: as in Fig. 1.

TABLE 2. Pelecaniform Bone Structure Results

Bone parameter	Vertebra		Anhinga	Phalacrocorax	Pelecanus	Kruskall-Wallis (*P*-value)
Adjusted cortical bone thickness (Cb.T)	Cervical	Mean ± SD	0.0106 ± 0.0045	0.0129 ± 0.0044	0.0050 ± 0.0019	0.009
		COV	0.4238	0.3422	0.3873	
	Thoracic	Mean ± SD	0.0099 ± 0.0024	0.0100 ± 0.0021	0.0046 ± 0.0007	0.003
		COV	0.2431	0.2137	0.1558	
Trabecular bone volume fraction (BV/TV)	Cervical	Mean ± SD	0.5393 ± 0.0943	0.4604 ± 0.1102	0.3404 ± 0.1748	0.073
		COV	0.1749	0.2393	0.5136	
	Thoracic	Mean ± SD	0.5747 ± 0.1098	0.3417 ± 0.0800	0.1540 ± 0.0371	0.001
		COV	0.1911	0.2341	0.2407	

TV when comparing cervical and thoracic vertebrae ($0.055 < P < 0.871$).

No significant differences in any of the bone structural parameters were observed among the charadriiform species examined (Fig. 3C,D). However, most species (*Uria*, *Fratercula*, and *Larus*) exhibited significantly thicker cortical bone in cervical vertebrae relative to thoracic vertebrae ($P < 0.01$; Fig. 3C). No differences in trabecular bone volume fraction were observed between the cervical and thoracic vertebrae for any charadriiforms ($0.078 < P < 0.522$).

DISCUSSION

Whereas the nature of interspecific differences in whole-body skeletal pneumaticity has been the subject of recent research (O'Connor, 2004, 2009; Smith, 2012), the impact of bone pneumatization on both structural and inferred functional characteristics remains much less well-characterized or understood. The only previous study (Fajardo et al., 2007) to examine structural differences at both the cortical and trabecular bone level indicated that apneumatic vertebrae in a representative diving anseriform bird had thicker cortical bone relative to a non-diving, size-matched pneumatic species. Notable differences in trabecular bone parameters (e.g., BV/TV) were virtually non-existent between the two taxa. The present study sought to characterize these two main bony structural attributes (Cb.T and trabecular BV/TV) in two other neognath clades in order to assess whether such patterns may apply to birds more generally. Representative pelecaniform (three species) and charadriiform (four species) birds were selected based on (1) the presence or absence of skeletal pneumaticity within vertebral elements and (2) different foraging strategies (subsurface diving foragers vs. flying/soaring foragers).

Bone Structure and Ecology in Extant Birds

Following Fajardo et al. (2007), this study predicted that birds with apneumatic vertebrae will have thicker cortical bone. The results for the pelecaniforms support this prediction, with the subsurface diving specialists (*Anhinga* and *Phalacrocorax*) exhibiting thicker cortical bone than the soaring *Pelecanus*. This is consistent with patterns among amniotes more generally, where thicker cortical bone has been interpreted to represent an anatomical specialization for diving (Olson and Hasegawa, 1979; Houssaye, 2009). By contrast, extreme pneumatization of vertebrae in the pelican results in relatively thin cortical bone, possibly related to a need for limiting mass increases in a large-bodied, soaring specialist (see, O'Connor, 2009).

In addition to cortical bone, this study also predicted a relatively high trabecular bone volume fraction in apneumatic vertebrae of diving forms, with a relatively low trabecular bone volume fraction in soaring taxa. Interestingly, this pattern was observed only in thoracic vertebrae of pelecaniforms, with the dedicated subsurface diving specialists *Anhinga* and *Phalacrocorax* having significantly higher BV/TV when compared to *Pelecanus*. However, there were no differences in BV/TV of cervical vertebrae within the pelecaniforms examined, indicating the presence of either site-specific responses to the pneumatization process (see O'Connor, 2009), or relatively high intraspecific variability within different regions of the vertebral column (see additional discussion below).

Unlike the pelecaniforms in this study (and anseriforms based on previous research; Fajardo et al., 2007), there were no clear relationships between pneumaticity and the examined bone structural parameters in charadriiform birds. This is interesting in that it suggests that at least one clade of neognath birds responds differently to the process of skeletal pneumatization, even in the face of superficially similar environmental challenges (i.e., subsurface dive foraging). Such differences may indicate a different bony response to the influence of the pneumatizing soft tissue (i.e., the pneumatic diverticulum), or may merely reflect clade-specific scaling relationships (or a combination thereof). Regarding the latter point, the absolute body sizes of pelecaniforms in the study sample (and of the clade more generally) is on average larger than that present in the charadriiforms. For comparative purposes with the results reported in this study, the mean body masses (554 g and 658 g) of the two anseriforms species examined by Fajardo et al. (2007) overlap the lower range of the charadriiforms in this study (Table 1).

Vertebral Location

This study found that pelicans (*Pelecanus*) have BV/TV values approaching 53% in cervical vertebrae, with BV/TV values in thoracic vertebrae maximally reaching 19%. Whereas the differences between BV/TV in cervical and thoracic vertebrae within the taxon are not significantly different ($P = 0.055$), this pattern suggests that vertebrae at different locations along the axial skeleton may be optimized for different functional demands. For example, the location of the vertebra within the neck may constrain the degree of trabecular

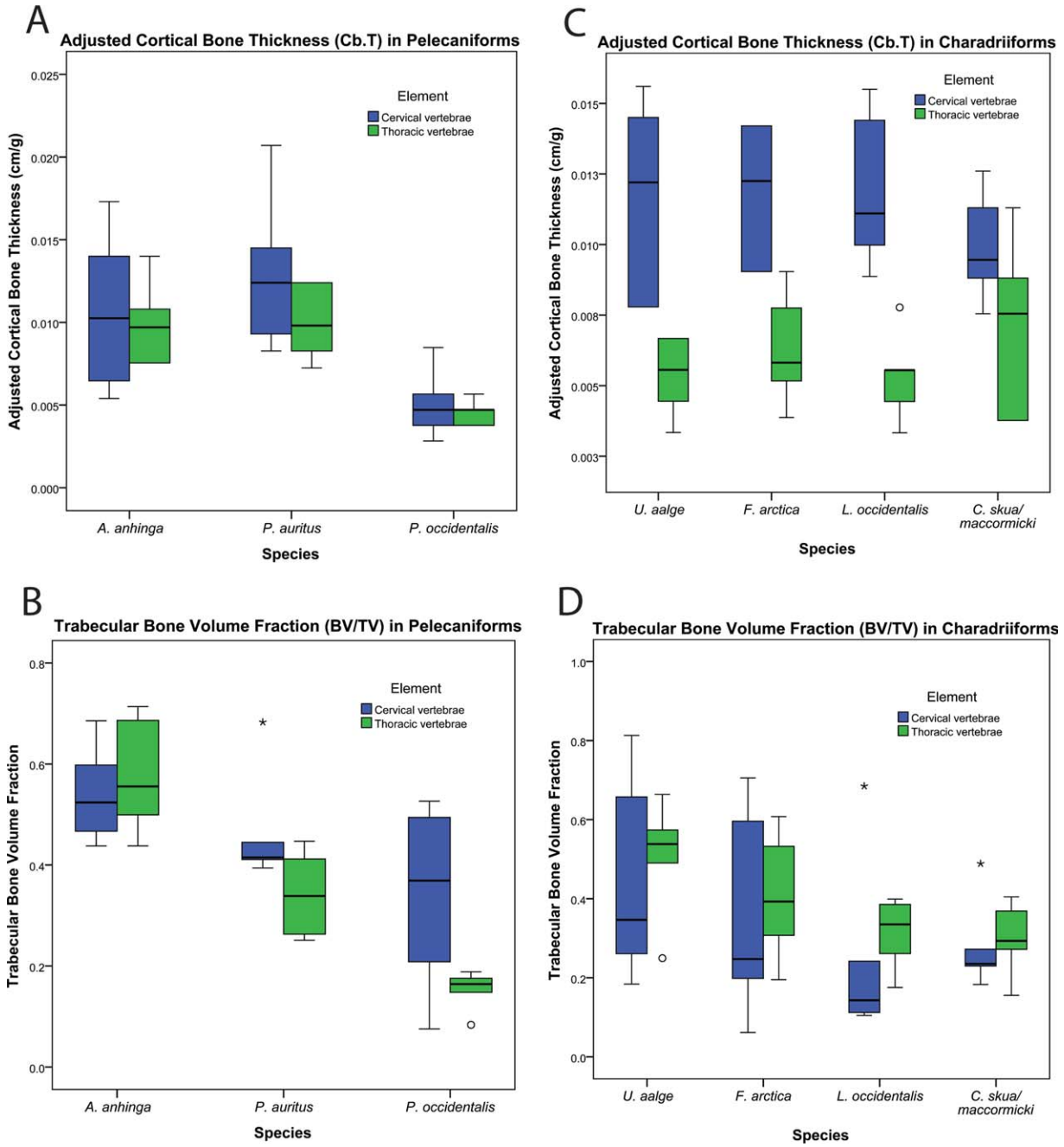

Fig. 3. Adjusted Cb.T. (**A**, **C**) and BV/TV (**B**, **D**) for pelecaniform (A,B) and charadriiform (C,D) birds.

bone resorption even in the presence of pneumatic invasion, as the extremely large head and long neck would no doubt produce high compressive stresses throughout the cervical series and at the junction of the neck and the trunk. Moreover, the increased degrees of freedom experienced by inter-cervical joints would also allow for more variably-oriented stresses throughout the cervical series, thereby further limiting how much bone could be reduced while retaining an appropriate safety margin. By contrast, thoracic vertebrae likely experience an entirely different and much more predictable loading environment due to their relative immobility (at least in birds) when compared to cervical vertebrae. Such a predicable loading environment is one that would allow resource focalization such that bone is placed where it is only absolutely necessary. Interestingly, the centra of human cervical vertebrae have been shown to exhibit greater bone mineral density than either thoracic or lumbar vertebrae (Weishaupt et al., 2001; Yoganandan et al., 2006), offering additional

TABLE 3. Charadriiform Bone Structure Results

Bone parameter	Vertebra		Uria	Fratercula	Larus	Catharacta	Kruskall–Wallis (*P*-value)
Adjusted cortical bone thickness (Cb.T)	Cervical	Mean ± SD	0.0117 ± 0.0033	0.0118 ± 0.0026	0.0118 ± 0.0026	0.0099 ± 0.0019	0.462
		COV	0.2809	0.2227	0.2192	0.1879	
	Thoracic	Mean ± SD	0.0054 ± 0.0013	0.0062 ± 0.0019	0.0054 ± 0.0015	0.0071 ± 0.0029	0.656
		COV	0.2419	0.3045	0.275	0.4126	
Trabecular bone volume fraction (BV/TV)	Cervical	Mean ± SD	0.4347 ± 0.2460	0.3427 ± 0.2521	0.2383 ± 0.2244	0.2741 ± 0.1090	0.209
		COV	0.566	0.7356	0.942	0.3976	
	Thoracic	Mean ± SD	0.5090 ± 0.1398	0.4047 ± 0.1580	0.3152 ± 0.0862	0.2979 ± 0.0871	0.091
		COV	0.2746	0.3904	0.2735	0.2925	

support for location-specific skeletal accommodations to functional demands.

Similarly in charadriiforms, the location of the vertebra along the column appears to influence pneumaticity–bone structure relationships. In *Uria*, *Fratercula*, and *Larus*, cervical cortical bone is significantly thicker than cortical bone in thoracic vertebrae. As observed in *Pelecanus*, the location of vertebrae within the neck may influence bone structural parameters for increased structural support, but in this case, it manifests as thicker cortical bone. It is possible that these two clades may utilize different mechanisms for maintaining/ensuring skeletal strength in this region, with one (*Pelecanus*) using trabecular bone and the other (charadriiforms) using cortical bone. In fact, relatively thick cortical bone may restrict the volume available for trabecular bone, resulting in cortical bone providing the bulk of structural support. However, this would only be a partial trade-off scenario, because relatively thin cortical bone may result in increased space for trabecular bone, but may not necessarily result in higher trabecular bone volume. Tommasini et al. (2005) found differing distributions of trabecular and cortical bone in lumbar vertebrae among different strains of inbred mice, yet the varying load-sharing compositions yielded similar mechanical stiffness at the whole vertebra level. Extending this concept to birds, a trade-off scenario in which structural support may be attained through either thick cortical bone or dense trabecular bone represents an additional hypothesis (i.e., one that was not the focus of the current research) that could be tested with future comparative work along these lines.

Intraspecific Variability and Methodology

The predicted relationships between pneumaticity and bone structure were not observed in BV/TV in cervical vertebrae of pelecaniforms, nor for either Cb.T or BV/TV in cervical and thoracic vertebrae of charadriiforms. The high degree of intraspecific variability (Tables 2 and 3) observed in these parameters may obscure any predicted patterns. For example, among pelecaniforms *Pelecanus* was expected to have less trabecular bone when compared to the other species. Whereas this prediction held for BV/TV within thoracic vertebrae, it did not for the cervical vertebra examined. And although this may represent a biologically significant signal, the absence of this expected pattern may be due to the highly variable BV/TV observed within cervical vertebrae in *Pelecanus* (CoV = 0.514). The high degree of intraspecific variability within *Pelecanus* (and other species examined) may be explained by several factors not accounted for in this study, such as age or sex of the individuals. In mammals, trabecular bone volume fraction is known to increase with age (Tanck et al., 2001; Wolschrijn and Weijs, 2004) and then decrease steadily after maturity through bone resorption (Mosekilde, 1989). It is unclear whether birds generally follow this mammalian pattern, but it is possible that variability of BV/TV within the study sample merely reflects the lack of age control inherent in comparative samples derived from museum collections. Similarly, sex-related differences may account for some of the intraspecific variability. It has been

demonstrated that during egg production female birds resorb metaphyseal trabecular (or "medullary") bone in limb elements as a source of calcium (Wilson and Thorp, 1998). As such, it is possible that the same response is present in vertebrae, potentially contributing to high bone volume fraction CoVs within the sample. Charadriiforms exhibited an even greater degree of intraspecific variability in bone structure than did the pelecaniforms (with CoV values as high as 0.942 in *Larus*). Like pelecaniforms, such high variability may be due to the factors discussed above that were not accounted for in this study (e.g., age, sex, etc.).

Overall, the results presented in this study did exhibit higher CoVs than those reported by Fajardo et al. (2007), a study in which the majority of the centrum was sampled. This may suggest that the location and/or size of the VOI selected for the BV/TV measurement did not adequately characterize the bone structure of the whole centrum. However, consistency in the pelecaniform thoracic BV/TV and the non-*Pelecanus* pelecaniform cervical BV/TV values suggests that trabecular bone was indeed defined appropriately and that the VOI was properly selected to reveal significant trends in bone structure and foraging strategy. As such, the high intraspecific variability observed in charadriiforms is most likely not an artifact of inappropriate bone definition or VOI selection, but instead reflects the normal range of variation within the clade or relates to one of the other factors (e.g., age or sex) previously discussed.

This study indicates that certain bone structural parameters (e.g., Cb.T), in addition to the relative extent of pneumaticity, both represent anatomical specializations related to foraging style. Certain species specializing in subsurface dive foraging exhibit apneumatic vertebrae and have thicker cortical bone and a higher site-specific trabecular bone volume fraction. This mirrors observations in other diving amniotes (including other bird groups specifically) and is consistent with the interpretation that such modifications serve to decrease buoyancy, allowing for greater energetic efficiency during diving. By contrast, nondiving flighted forms, particularly those exhibiting specialized flight behaviors (e.g., soaring) and pneumatic vertebrae, tend to have thinner cortical bone and lower relative trabecular bone volume fraction. Such modifications may work to constrain body mass increases, while allowing for larger body sizes (i.e., volumes). This has been referred to as volume-mass decoupling (O'Connor, 2009) and would serve to increase energetic efficiency in volant forms, particularly those that do not engage in specialized subsurface diving behaviors.

Finally, it is also possible, if not probable, that the location of the vertebra along the axial column constrains the nature of responses during pneumatization, as functional demands may dictate site-specific responses. For example, both diving and flying specialists may require thicker cortical bone or higher trabecular bone volume fraction in vertebrae at the base of the neck in order to resist relatively higher compressive strains associated with supporting the weight of the head and neck. Moreover, aerial diving specialists may benefit from this increased structural support in cervical vertebrae at the moment of impact with the surface of the water during diving. One example from the appendicular skeleton that supports the functional demands hypothesis (rather than some systemic influence) is the occurrence of differential pneumatization in femora of pelecaniforms. *Pelecanus* is unique among the large-bodied, hyperpneumatic soaring birds (O'Connor, 2009) in exhibiting an apneumatic femur in the presence of pneumatic distal hind limb elements (e.g., tibiotarsus). This is significant for the discussion here in that the femur in *Pelecanus* maintains a close association with pneumatic diverticula, particularly around the hip joint. Thus, the fact that the femur is not pneumatic strongly suggests that location (or element) specific functional demands do influence pneumaticity states and any associated biomechanical sequelae of the pneumatization process. The results presented herein suggest that future studies take into account a more-detailed consideration of ontogenetic, sex-specific, and functional factors that potentially drive high levels of intraspecific variability in these osteological characteristics.

ACKNOWLEDGEMENTS

Authors would like to thank the following individuals for access to specimens: W. and B. Fox (Pelican Harbor Seabird Station), B. Livezey and S. Rogers (Carnegie Museum of Natural History), and J. Dean and C. Milensky (Smithsonian Institution National Museum of Natural History). For training at the Ohio University μCT facility, S.G. thanks R. Ridgely.

LITERATURE CITED

Benson RBJ, Butler RJ, Carrano MT, O'Connor PM. 2012. Air-filled postcranial bones in theropod dinosaurs: physiological implications and the 'reptile'-bird transition. Biol Rev 87:168–193.

Bellairs AA, Jenkin CR. 1960. The skeleton of birds. In: Marshall J, editor. Biology and comparative physiology of birds. New York: Academic Press. p 241–300.

Boas JEV. 1929. Biologisch-anatomische Studien über den Hals der Vögel. Kgl Danske Vidensk Selsk Skr Naturvidensk Mathem Afd 9:105–222.

Bremer JL. 1940. The pneumatization of the humerus in the common fowl and the associated activity of theelin. Anat Rec 77:197–211.

Carrano MT, O'Connor PM. 2005. Bird's eye view. Nat Hist 114:42–47.

Claessens LPAM, O'Connor PM, Unwin DM. 2009. Respiratory evolution facilitated the origin of pterosaur flight and aerial gigantism. PLoS One 4:e4497.

Cotter MM, Scott SW, Latimer BM, Hernandez CJ. 2009. Trabecular microarchitecture of hominoid thoracic vertebrae. Anat Rec 292:1098–1106.

Cruz-Orive LM, Karlsson LM, Larsen SE, Wainschtein F. 1992. Characterizing anisotropy: a new concept. Micron Microscopica Acta 23:75–76.

Cubo J, Casinos A. 1999. Incidence and mechanical significance of pneumatization in the long bones of birds. Zool J Linn Soc 130:499–510.

Currey JD, Alexander RM. 1985. The thickness of the walls of tubular bones. J Zool Lond (A) 206:453–468.

Duncker H-R. 1971. The lung air sac system of birds. Adv Anat Embryol Cell Biol 45:1–171.

Duncker H-R. 2004. Vertebrate lungs: structure, topography and mechanics: a comparative perspective of the progressive integration of respiratory system, locomotor apparatus and ontogenetic development. Respir Physiol Neurobiol 144:111–124.

Dunning JB. 2007. CRC handbook of avian body masses. Boca Raton: CRC press. p 672.

Fajardo RJ, Hernandez E, O'Connor PM. 2007. Postcranial skeletal pneumaticity: a case study in the use of quantification microCT to assess vertebral structure in birds. J Anat 211:138–147.

Hogg DA. 1984. The distribution of pneumatisation in the skeleton of the adult domestic fowl. J Anat 138:617–629.

Houssaye A. 2009. "Pachyostosis" in aquatic amniotes: a review. Integr Zool 4:325–340.

Kafka V. 1983. On hydraulic strengthening of bones. Biorheology 20:789–793.

Ketcham RA, Ryan TM. 2004. Quantification and visualization of anisotropy in trabecular bone. J Microsc 213:158–171.

Mosekilde L. 1989. Sex differences in age-related loss of vertebral trabecular bone mass and structure—biomechanical consequences. Bone 10:425–432.

O'Connor PM. 2004. Pulmonary pneumaticity in the postcranial skeleton of extant aves: a case study examining Anseriforms. J Morphol 261:141–161.

O'Connor PM. 2006. Postcranial pneumaticity: an evaluation of soft-tissue influences on the postcranial skeleton and the reconstruction of pulmonary anatomy in archosaurs. J Morphol 267:1199–1226.

O'Connor PM. 2009. Evolution of archosaurian body plans: skeletal adaptations of an air-sac-based breathing apparatus in birds and other archosaurs. J Exp Biol A 311:504–521.

Olson SL, Hasegawa Y. 1979. Fossil counterparts of giant penguins from the north pacific. Science 206:688–689.

Ridler TW, Calvard S. 1978. Picture thresholding using an iterative selection method. IEEE Trans Syst Man Cybern 8:630–632.

Sander PM, Klein N, Buffetaut E, Cuny G, Suteethorn V, Le Loeuff J. 2001. Biology of the sauopod dinosaurs: the evolution of gigantism. Biol Rev 86:117–155.

Schepelmann K. 1990. Erythropoietic bone marrow in the pigeon: development of its distribution and volume during growth and pneumatization of bones. J Morphol 203:21–34.

Schwarz-Wings D, Meyer CA, Frey E, Manz-Steiner H-R, Schumacher R. 2010. Mechanical implications of pneumatic neck vertebrae in sauropod dinosaurs. Proc R Soc B 277:11–17.

Smith ND. 2012. Body mass and foraging ecology predict evolutionary patterns of skeletal pneumaticity in the diverse "Waterbird" clade. Evolution 66:1059–1078.

Smith TD, Rossie JB, Cooper GM, Mooney MP, Siegel MI. 2005. Secondary pneumatization of the maxillary sinus in callitrichid primates: insights from immunohistochemistry and bone cell distribution. Anat Rec A 285:677–689.

Tanck E, Homminga J, Van Lenthe GH, Huiskes R. 2001. Increase in bone volume fraction precedes architectural adaptation in growing bone. Bone 28:650–654.

Tommasini SM, Morgan TG, Van der Meulen MCH, Jepsen KJ. 2005. Genetic variation in structure–function relationships for the inbred mouse lumbar vertebral body. J Bone Min Res 20:817–827.

Wedel MJ. 2003. Vertebral pneumaticity, air sacs, and the physiology of sauropod dinosaurs. Paleobiology 29:243–255.

Wedel MJ. 2005. Postcranial skeletal pneumaticity in sauropods and its implications for mass estimates. In: Curry Rogers KA, Wilson JA, editors. The Sauropods: evolution and paleobiology. Berkeley: UC Press. p 201–228.

Weishaupt D, Schweitzer ME, DiCuccio MN, Michael N, Whitley PE. 2001. Relationships of cervical, thoracic, and lumbar bone mineral density by quantitative CT. J Comput Assist Tomogr 25:146–150.

Wilson S, Thorp BH. 1998. Estrogen and cancellous bone loss in the fowl. Calcif Tissue Int 62:506–511.

Witmer LM. 1990. The craniofacial air sac system of Mesozoic birds (Aves). Zool J Linn Soc 100:327–378.

Wolschrijn CF, Weijs WA. 2004. Development of the trabecular structure within the ulnar medial coronoid process of young dogs. Anat Rec A 278:514–519.

Yoganandan N, Pintar FA, Stemper BD, Baisden JL, Aktay R, Shender BS, Paskoff G. 2006. Bone mineral density of human female cervical and lumbar spines from quantitative computed tomography. Spine 3:73–76.

Zusi RL. 1962. Structural adaptations of the head and neck in the black skimmer, *Rynchops nigra*. Pub Nut Ornith Club 3:1–101.

APPENDIX: RAW VALUES OF MEASURED BONE PARAMETERS

Order	Species	ID	Cervical Cb.T (cm/g)	Thoracic Cb.T (cm/g)	Cervical BV/TV	Thoracic BV/TV
Pelecaniforms	*Anhinga anhinga*	CM13826	0.0173	0.0108	0.5979	0.5143
	Anhinga anhinga	CM14362	0.0140	0.0097	0.4376	0.5969
	Anhinga anhinga	CM13811	0.0097	0.0097	0.5663	0.4994
	Anhinga anhinga	CM14313	0.0065	0.0075	0.4669	0.4377
	Anhinga anhinga	USNM500870	0.0054	0.0075	0.6856	0.7136
	Anhinga anhinga	USNM500869	0.0108	0.0140	0.4815	0.6863
	Phalacrocorax auritus	OUVC9772	0.0145	0.0124	0.4109	0.4471
	Phalacrocorax auritus	OUVC10234	0.0083	0.0083	0.4450	0.3113
	Phalacrocorax auritus	OUVC10291	0.0093	0.0093	0.4150	0.2630
	Phalacrocorax auritus	OUVC10482	0.0124	0.0072	0.4147	0.4118
	Phalacrocorax auritus	USNM561412	0.0124	0.0124	0.3941	0.2509
	Phalacrocorax auritus	USNM560265	0.0207	0.0103	0.6829	0.3661
	Pelecanus occidentalis	OUVC10433	0.0038	0.0047	0.3175	0.0836
	Pelecanus occidentalis	OUVC10484	0.0047	0.0047	0.5262	0.1757
	Pelecanus occidentalis	OUVC10478	0.0085	0.0038	0.4941	0.1630
	Pelecanus occidentalis	OSUM2576	0.0057	0.0038	0.4206	0.1655
	Pelecanus occidentalis	USNM553693	0.0028	0.0057	0.0754	0.1885
	Pelecanus occidentalis	USNM621490	0.0047	0.0047	0.2084	0.1478
Charadriiforms	*Uria aalge*	CM399	0.0122	0.0044	0.2608	0.2495
	Uria aalge	CM3958	0.0156	0.0067	0.1840	0.5297
	Uria aalge	CM14348	0.0078	0.0056	0.3214	0.5738
	Uria aalge	CM11557	0.0078	0.0056	0.8131	0.5468
	Uria aalge	CM14180	0.0145	0.0033	0.6574	0.4906
	Uria aalge	CM11930	0.0122	0.0067	0.3716	0.6637
	Fratercula arctica	CM11726	0.0090	0.0052	0.2029	0.1950
	Fratercula arctica	CM398	0.0142	0.0039	0.2918	0.3075
	Fratercula arctica	CM11794	0.0142	0.0065	0.7055	0.4752
	Fratercula arctica	USNM18055	0.0142	0.0090	0.1985	0.5323
	Fratercula arctica	USNM623288	0.0103	0.0052	0.5958	0.6077
	Fratercula arctica	USNM623289	0.0090	0.0077	0.0615	0.3102
	Larus occidentalis	CM12321	0.0089	0.0044	0.2416	0.1755
	Larus occidentalis	CM11106	0.0100	0.0055	0.1586	0.3666
	Larus occidentalis	CM11757	0.0111	0.0033	0.6849	0.3991
	Larus occidentalis	CM11776	0.0155	0.0078	0.1121	0.3853
	Larus occidentalis	CM11758	0.0111	0.0055	0.1048	0.3037
	Larus occidentalis	CM11756	0.0144	0.0055	0.1276	0.2612
	Catharacta skua	CM11606	0.0113	0.0075	0.2385	0.1558
	Catharacta skua	CM10116	0.0126	0.0038	0.2323	0.3686
	Catharacta skua	USNM576076	0.0075	0.0113	0.2722	0.4046
	Catharacta skua	USNM623300	0.0101	0.0075	0.4888	0.3116
	Catharacta maccormicki	USNM491325	0.0088	0.0038	0.1829	0.2750
	Catharacta maccormicki	USNM554803	0.0088	0.0088	0.2299	0.2720